Journal of Materials and Environmental Sciences
ISSN : 2028-2508

JMES, 2017 Volume 8, Issue 3, Page 911-920

http://www.jmaterenvironsci.com

ICMES2016, 1-3 Dec. 2016,

Simultaneous effect of electric field and temperature on bound exciton states in semiconductor quantum dot

El Hadi M.[1], El Moussaouy A.[1,2], Nougaoui A.[1], Bria D.[1]

1. Laboratoire de Dynamique et d'Optique des Matériaux, Département de Physique, Faculté des Sciences, Université Mohammed I, 60000, Oujda, Maroc
2. Centre Régional des Métiers de l'Education et de la Formation, 60000, Oujda, Maroc

Received 4 Dec 2016,
Revised 30 Jan 2017,
Accepted 31 Jan 2017,

Keywords

- ✓ Quantum dots;
- ✓ Exciton;
- ✓ Electric field;
- ✓ Temperature;
- ✓ Photoluminescence

A. El Moussaouy
azize10@yahoo.fr
+212 536 50 06 01/02

Abstract

The present study seeks to scrutinize theoretically the role of simultaneous effect of electric field and temperature on the exciton binding energy and photoluminescence energy in a cylindrical quantum dot (QD). Using a variational approach and the correlation between the electron and the hole in the trial wave function within the effective-mass approximation, we calculate the exciton binding energies of the ground state and photoluminescence energies as the function of the geometry, the temperature and the strength of the applied electric field along the growth direction of the cylinder. Our numerical findings for $GaAs/Ga_{(1-x)}Al_{(x)}As$ have shown that, for each temperature value, both the binding energy and the photoluminescence energy are decreasing functions of the electric field strength. Given a fixed electric field strength, both quantities then becomes decreasing functions of the temperature. More especially, we have found that the exciton binding energy is decreasing function of the QD height with and without electric field and temperature effects. Furthermore, in the presence of these influences, it is shown that the Stark effect for the ground state becomes important when increasing QD height.

1. Introduction

In recent years, much attention was paid to the investigation of the physics of low dimensional semiconductor structures. Many theoretical and experimental studies have been carried out to understand the electronic and optical properties of fewer particles in the quantum wells (QWs), quantum well wires (QWWs) and quantum dots (QDs) [1–15]. This interest is mainly for their present and future applications in practice as a variety of optoelectronic devices, such as QD lasers [16], QD infrared detectors [17], QD memory devices [18], and single-electron transistors [19]. The QDs structures seem to be most promising, for the particles in these systems are confined in all the three spatial dimensions, which bring in pronounced quantum effects when the electron wave length becomes comparable to the confinement length.

The works on excitons in QDs structures are relevant for the understanding of some of their physical properties. In consequence, there has been growing interest in the topic regarding different aspects of excitonic effects in various nanostructures (See, for instance, Refs. [20–27]). Le Goff and Stébé [20] have presented a model for the description of excitons in cylindrical QD semiconductor by examining both the dependence of longitudinal and lateral confinement on excitonic properties. Wang and Guo [21] have investigated the excitonic effects on third-harmonic-generation coefficient for disk-like parabolic QD. Szafran et al. [22] have studied the dissociation of excitons and trions in vertically coupled QDs. Chwiej et al. [23] have examined the Coulomb-driven Stark effect anomaly for an exciton in the same QD systems. Szafran et al. [24] have considered the horizontal field orientation and non aligned dots in the investigation of Stark effect on the exciton spectra of vertically coupled double disk-shaped QD with smooth walls. Barticevic et al. [25] have obtained the energy spectra of exciton states in disk-shaped QD under growth-direction magnetic fields. Szafran et al. [26] have examined the excitonic spectra in vertical stacks of perfectly aligned triple and quadruple QD with individual disk-shaped

quantum well (QW) profiles for the confinement potential. Wang et al. have presented in Ref. [27] a study on the effect of tilted electric field on the magnetoexciton ground state of cylindrical QD.
Furthermore, recently, much experimental and theoretical works have been devoted to the understanding of the excitons and impurities states and related optical properties in the QDs by using the external perturbations [28-38]. Erdogan et al. [28] have calculated the temperature effect on the donor binding energy, self-polarization, and electric field polarization in a $GaAs/Ga_{(0.7)}Al_{(0.3)}As$ spherical QD with off center donor impurity under the action of electric field and hydrostatic pressure. By using the configuration-integration method, Jian-Hui Yuan et al. [29] have investigated theoretically the low-lying states and optical absorption properties of a hydrogenic impurity in a parabolic QD modulation by applied electric field. Some of us [35-38] have investigated the properties of excitons and impurities under action of external perturbations in cylindrical semiconductors QDs.
More interest, in the area of low-dimensional semiconductor structures devices, have been focused on the study of an electric field effect on the spectrum of localized states in semiconducting nanostructure. The role of an applied external electric field gives rise to polarization of the carrier's distribution and to energy shift of the quantum state. The electric field effect reflects in a change in the carrier confinement profiles of the conduction and valence band potential energies. Since the electrons and holes have opposite charges, the action of the electric field on them implies an increase in the average value of the electron–hole distance. Therefore, one should expect that an influence on the excitonic properties will appeared, which could be used to control and modulate the intensity of output of optoelectronic devices [39] and making electric field an effective tool for examining the physical properties of these structures, both from theoretical and experimental points of view. Thus, the external electric field effects on the hydrogenic impurity and excitonic states of QDs have been studied in several works [40–48]. All of the works mentioned above have shown that the impurity and the exciton states considerably depend on the QD parameters and the applied electric field strength. Recently, Leon et al. [49] have presented an analytical solution of the Schrödinger equation in prolate spheroidal coordinates to examine the electronic and excitonic states in ellipsoidal and semi-ellipsoidal infinite potential QDs, as a function of the dot size. More recently, Mora-Ramos et al. [50] have investigated the effect of applied electric field in $GaAs/Ga_{(1-x)}Al_{(x)}As$ QD. In addition, the effects of the temperature also modify the semiconductor band structure and lead to changes in the properties of the elementary excitations of the QDs. The application of temperature can provide much valuable information about the semiconductor. This perturbation can be modified the electronic structure, affecting the variation of the static dielectric constant of the crystal. Many works have interested to the effect of temperature on the excitons in nanostructures [51-53]. Xie [51] has discussed the temperature and hydrostatic pressure effects of an exciton–donor complex in a $GaAs/AlAs$ disc-like QD.Tan Man et al. [52] have studied the temperature-dependent thermal escape and Auger recombination coefficients in CdTe/ZnTe QD. Duque et al. [53] have investigated the linear and nonlinear optical properties of exciton in QD with the form of a disc under the influence of temperature and pressure.
To the best of our knowledge, the simultaneous effect of external electric field and temperature on the exciton coupled states and photoluminescence of cylindrical QDs have not been investigated before. To this end, we study the problem of excitonic states of these systems, under simultaneous influence of an external electric field and temperature in the framework of effective-mass approximation and variational procedure. In this regard, we performed detailed theoretical investigations on the excitonic binding energy distributions and photoluminescence energy transition in cylindrical QD, considering an applied electric field and temperature. We use in the numerical calculation the $GaAs/Ga_{(1-x)}Al_{(x)}As$ compounds, assuming a finite confinement potential. The results show the competing influences of the geometrical confinement, the electric field and temperature.
The paper is organized as follows: in Section 2 we present the theoretical framework of an effective Hamiltonian for the exciton ground state in cylindrical coordinates with finite potential well, and the variational calculation for the exciton state binding energy. The numerical results and a detailed discussion are performed in Section 3. Finally, the main results are summarized in Section 4.

2. Formalism

For our theoretical modeling, the QD is assumed to have a cylindrical form of radius R and height $H = 2d$ and is made of a GaAs semiconductor material surrounded by $Ga_{(1-x)}Al_{(x)}As$ compound, whose prototypical scheme and potential energy profile are those shown in Figure 1. In the presence of applied electric field and temperature, the basic Hamiltonian for exciton states in cylindrical QD can be written within the framework of the effective-mass and non-degenerate band approximation, as follows:

$$H = -\frac{\hbar^2}{2m_e^*}\nabla_e^2 - \frac{\hbar^2}{2m_h^*}\nabla_h^2 - \frac{e^2}{\varepsilon_0(T)|r_e - r_h|} + V_w^e(r_e, T) + V_w^h(r_h, T) + eF(z_e - z_h)\,, \quad (1)$$

Where m_e^* and m_h^* are the effective masses of the electron and hole, respectively. $r_e = (\rho_e, z_e)$ and $r_h = (\rho_h, z_h)$ are the spatial coordinates of the electron and hole in cylindrical frame, respectively.

$-\frac{e^2}{\varepsilon_0(T)|r_e - r_h|}$ is the Coulomb potential, where $\varepsilon_0(T)$ is the static dielectric constant at temperature T. F is the electric field oriented along the Z-axis and e is the absolute value of the electron charge.The temperature dependent static dielectric constant is written as:

$$\varepsilon_0(T) = \varepsilon_a e^{\alpha_1 T}\,, \quad (2)$$

where for $T < 200\ K$ we have $\varepsilon_a = 12.6498$, $\alpha_1 = 9.4 \times 10^{-5} K^{-1}$,

whereas for $T \geq 200$ K we have $\alpha_1 = 20.4 \times 10^{-5} K^{-1}$.

$V_w^e(r_e, T)$ ($V_w^h(r_h, T)$) is the corresponding electron (hole) confining potential at temperature T expressed as follows :

$$V_w(r, T) = \begin{cases} 0 & \text{if } \rho_i \leq R \text{ and } |Z_i| \leq d\,, \\ V_i(T) & \text{otherwise.} \end{cases} \quad (3)$$

We can write the expressions of $V_e(x, T)$ and $V_h(x, T)$ as follows [54] $V_e(x, T) = 0.658\Delta E_g(x, T)$ and $V_h(x, T) = 0.342\Delta E_g(x, T)$. $\Delta E_g(x, T)$ is the band gap difference between dot and barrier materials as a function of temperature given by [55] :

$$\Delta E_g(x, T) = \Delta E_g(x) - T(1.11 \times 10^{-4}).x\,, \quad (4)$$

Where $\Delta E_g(x) = E_{g_{Ga(1-x)Al(x)As}}(x) - E_{g_{GaAs}}(x) = 1.155x + 0.37x^2$. (5)

The effective Hamiltonian, in the atomic units system ($a_{ex}^* = \frac{\varepsilon_0(0)\hbar^2}{\mu e^2}$ excitonic Bohr radius and Rydberg energy $R_{ex}^* = \frac{\mu e^2}{2\varepsilon_0^2(0)\hbar^2}$), reads:

$$H_{eff} = -\frac{1}{1+\sigma}\left[\frac{\partial^2}{\partial \rho_e^2} + \frac{1}{\rho_e}\frac{\rho_{eh}^2 + \rho_e^2 - \rho_h^2}{\rho_e \rho_{eh}}\frac{\partial^2}{\partial \rho_e \rho_{eh}} + \frac{\partial^2}{\partial z_e^2}\right]$$
$$-\frac{1}{1+\sigma}\left[\frac{\partial^2}{\partial \rho_h^2} + \frac{1}{\rho_h}\frac{\rho_{eh}^2 + \rho_h^2 - \rho_e^2}{\rho_h \rho_{eh}}\frac{\partial^2}{\partial \rho_h \rho_{eh}} + \frac{\partial^2}{\partial z_h^2}\right] - \left[\frac{\partial^2}{\partial \rho_{eh}^2} + \frac{1}{\rho_{eh}}\frac{\partial}{\partial \rho_{eh}}\right]$$
$$-\frac{\varepsilon_0(0)}{\varepsilon_0(T)}\frac{2}{\sqrt{\rho_{eh}^2 + (z_e - z_h)^2}} + V_w^e(z_e, T) + V_w^h(z_h, T) + eF(z_e - z_{h)}\,, \quad (6)$$

where $\sigma = \frac{m_e^*}{m_h^*}$.

In order to calculate the exciton binding energy, we choose the following wave function [20,50]:

$$\psi_{ex}(\rho_e, \rho_h, z_e, z_h, T) = F_e(\rho_e, z_e, T)F_h(\rho_h, z_h, T)F_{eh}(\rho_{eh}, |z_e - z_h|), \quad (7)$$

with $F_{eh}(\rho_{eh}, |z_e - z_h|) = \exp(-\alpha\rho_{eh})\exp(-\gamma(z_e - z_h)^2)\,(1 + F\beta(z_e - z_h))$, (8)

and $F_i(\rho_i, z_i, T) = f_i(\rho_i, T)g_i(z_i, T), \qquad (i = e, h).$ (9)

Respectively, the corresponding 2D (lateral direction) and 1D (longitudinal direction) effective mass Schrödinger equations are:

$$\left\{-\frac{\hbar^2}{2m_i^*}\nabla_i^2 + V_w^i(\rho_i, T)\right\} f_i(\rho_i, T) = E_i(\rho_i) f_i(\rho_i, T), \quad (i = e, h)\,, \quad (10)$$

$$\left\{-\frac{\hbar^2}{2m_i^*}\nabla_i^2 + V_w^i(z_i, T)\right\} g_i(z_i, T) = E_i(z_i) g_i(z_i, T), \quad (i = e, h). \quad (11)$$

With solutions of the form:

$$f_i(\rho_i, T) = \begin{cases} J_0(\theta_i(T)\frac{\rho_i}{R}) & \text{for } \rho_i \le R\,, \\ A_i(T)K_0(\beta_i(T)\rho_i) & \text{for } \rho_i > R \quad (i = e, h), \end{cases} \tag{12}$$

$$g_i(z_i, T) = \begin{cases} \cos(\pi_i(T)\frac{z_i}{2d}) & \text{for } |z_i| \le d \\ B_i(T)\exp(k_i(T)|z_i|) & \text{for } |z_i| > d \quad (i = e, h). \end{cases} \tag{13}$$

J_0 and K_0 are the modified Bessel functions of 0th order. $\theta_i(T), \beta_i(T), \pi_i(T), k_i(T), A_i(T)$ and $B_i(T)$ are determined from the following equations, which are obtained from the boundary conditions at the interfaces $\rho_i = R$ and $|z_i| = d$.

$$A_i(T) = J_0(\theta_i(T))/K_0(\beta_i(T)R), \tag{14}$$

$$\theta_i(T)\, J_1(\theta_i(T))/J_0(\theta_i(T)) = \beta_i(T)RK_1(\beta_i(T)R)/K_0(\beta_i(T)R), \tag{15}$$

$$B_i(T) = \cos(\pi_i(T)/2)/\exp(-k_i(T)d)\,, \tag{16}$$

$$\tan(\pi_i(T)/2) = k_i(2d/\pi_i(T))\,. \tag{17}$$

In Eq. (8), α, β and γ are variational parameters. The binding energy of the exciton system is given by:

$$E_B(F, T) = E_l(F, T) - E_G(F, T), \tag{18}$$

where $E_l(F, T)$ and $E_G(F, T)$ are, respectively, the lowest energy and the exciton ground-state energy which can be written as:

$$E_l(F, T) = E_e(F, T) + E_h(F, T), \tag{19}$$

$$E_G(F, T) = \min_{\alpha,\beta,\gamma}\langle\psi_{ex}|H_{eff}|\psi_{ex}\rangle. \tag{20}$$

$E_e(F, T)$ and $E_h(F, T)$ are the free electron and hole energies.

The value of the electron–hole distance is written as:

$$z_{eh} = \left[\langle\psi_{ex}|(z_e - z_h)^2|\psi_{ex}\rangle\right]^{1/2}. \tag{21}$$

We define the normalized photoluminescence energy transition (PL) by subtracting the GaAs energy gap from the quantity [50]:

$$E_e + E_h + E_{gap} - E_G\,, \tag{22}$$

Where E_e and E_h are, respectively, the confined ground state energy of the electron and hole and E_{gap} is the GaAs bandgap. The stark shift on the exciton is obtained as:

$$\Delta E_B = E_B(F) - E_B(F = 0). \tag{23}$$

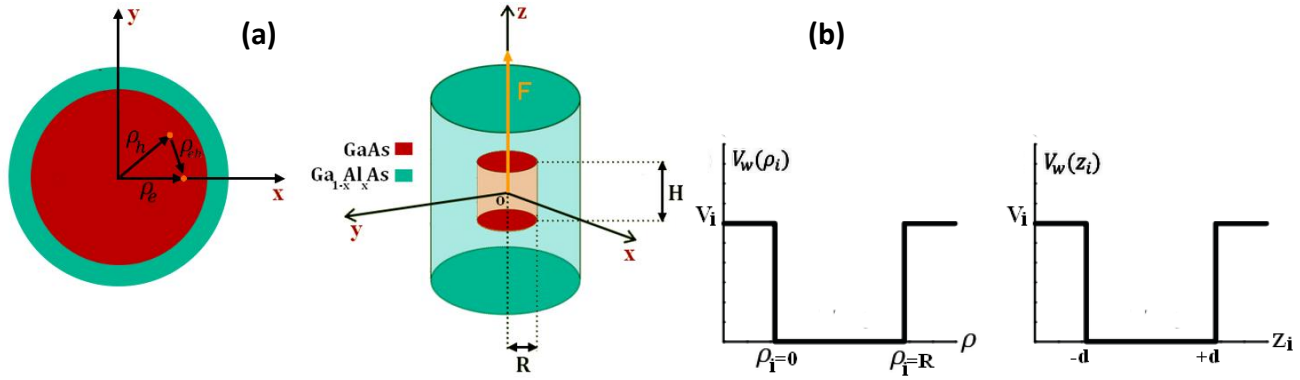

Figure 1: Schematic representation of the cylindrical QD considered in the present work. Graphs (a) show, the self-assembled $GaAs/Ga_{(1-x)}Al_{(x)}As$ QD under investigation with the dot height H and the radius R in the presence of an electric field F, and the electron and hole positions. Schematic representations of the radial and axial confinement potentials are depicted in Graphs (b).

3. Numerical Results and Discussions

In the following, we have performed the numerical computations for the exciton binding energy of the ground state in a cylindrical QD made of GaAs embedded in $Ga_{(1-x)}Al_{(x)}As$ material. The electric field and temperature dependence of the binding energy, by including the interaction between the electron and hole, are obtained numerically by evaluating different kinds of triple and double integrals over the GaAs QD and the

$Ga_{(1-x)}Al_{(x)}As$ matrix spaces.The integrals are evaluated with a step adaptive iterative method. Then the value of the electric field and temperature are set up and the corresponding energies are found by iterations until a convergence better than 0.1 was attained. Our numerical results are presented in units of the effective Rydberg energy $R^*_{ex} = 3$ meV and the effective Bohr radius $a^*_{ex} = 183.431$ Å, which are evaluated at zero temperature. In Figure 2 we have presented the variation of the exciton binding energy in a cylindrical QD in the situation of fixed radius ($R = 1a^*_{ex}$) as a function of the height H of the cylinder. The curves are obtained for three different values of the applied electric field along the z-direction at low and room temperature (T=0 and 300 K). For each curve, the binding energy increases as the height reduces, reach a maximum, and then decreases, which is qualitatively similar to our previous works [38]. Besides, the shapes of the curves obtained are similar. At small height values, discrete levels are absent in the well, and the exciton particle wave functions are distributed outside the QD. Further, as the electric field is increased the electron is pulled towards one side of the QD, resulting the overall decrease of the binding energies. Moreover, we notice that the binding energy is more significant for dots of smaller heights than the larger dot heights due to the confinement. In addition, the temperature effect on the binding energy is qualitatively similar to the electric field effect. We remark that the exciton binding energy decreases with a raise in the temperature, but less important than the effect of electric field. We notice that the exciton becomes less stable when applying electric field, at high temperature.
Likewise, the variation of the exciton binding energy with the electric field strength shows an overall decreasing dependence. In Figure 3 we have presented the variation of the binding energy as a function of applied electric field for two values of the QD height, namely,$H = 0.5$ and $1\ a^*_{ex}$, at zero and room temperature. We notice that by fixing the dot radius, the binding energy grows with the reduction of the cylinder height, due to the rise in the electron and hole confinement. In the same situation, we detect that the effect of applied electric field is very weak, for smaller cylinder height H, and becomes more influential for higher values of the QD size. In addition, we remark in this figure that the exciton binding energy decreases by increasing the temperature, and this decrease becomes more important for large values of the QD height. These results are in good agreement with those obtained by Mora-Ramos [50] at low temperature limit.

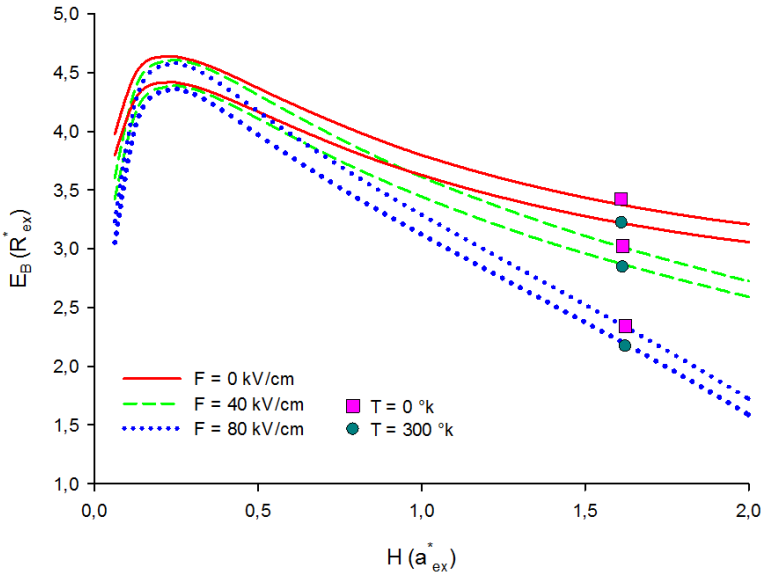

Figure 2: Binding energy of an exciton confined in a cylindrical $Ga_{(1-x)}Al_{(x)}As$ QD, of radius $R = 1\ a^*_{ex}$, as a function of the height H for three different values of the electric field (F = 0 kV/cm, (solid lines) 40 kV/cm, (dashed lines) 80 kV/cm, (dotted lines)), at zero and room temperature.

To more understand the effect of temperature on exciton properties, we have plotted, in Figure, 4 the exciton binding energy as a function of the temperature in a QD of radius $R = 1\ a^*_{ex}$ and height $H = 1\ a^*_{ex}$ when theelectric field of F = 0, 40 and 80 kV/cm are applied. This figure shows that, for each electric field value, the exciton binding energy decreases with increasing temperature, which is qualitatively similar to the work in Ref [48]. This temperature dependence of the exciton binding energy has been examined in two different temperature regimes. At low temperature regime, T < 200 K, the exciton binding energy almost linearly decreases more slowly than that at high temperature regime, T > 200 K. This is due to the difference between the temperature coefficients in the dielectric constants, for two temperature regimes, Eq. (2).

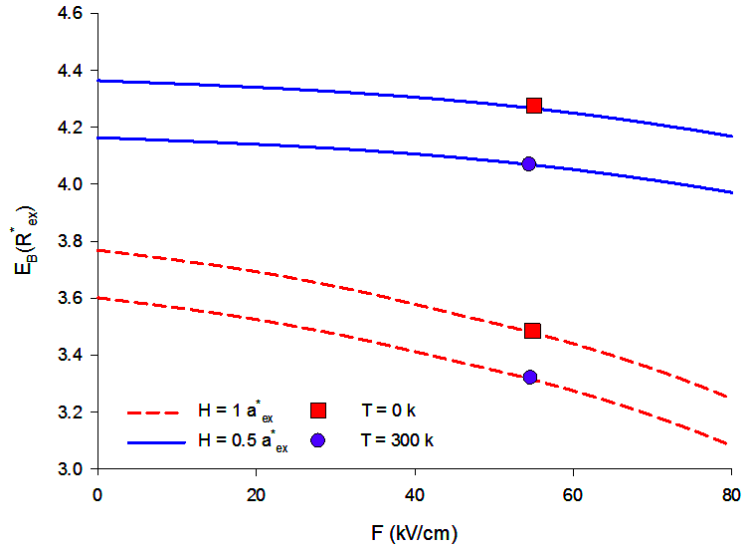

Figure 3: Variation of the exciton Binding energy in a cylindrical $Ga_{(1-x)}Al_{(x)}As$ QD, of radius $R = 1\ a^*_{ex}$, as a function of applied electric field for two values of the QD height ($H = 0.5\ a^*_{ex}$ and $H = 1\ a^*_{ex}$)at zero and room temperature.

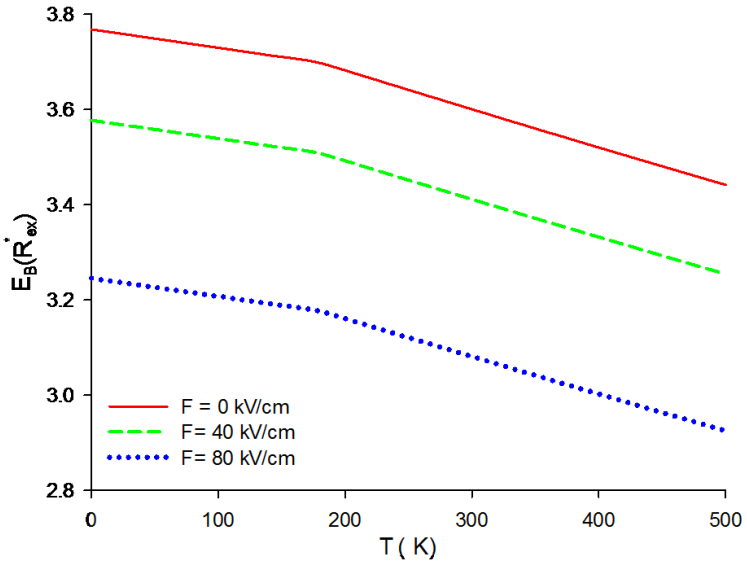

Figure 4: Variation of the exciton binding energy in a cylindrical $Ga_{(1-x)}Al_{(x)}As$ QD of radius $R = 1\ a^*_{ex}$ and height $H = 1\ a^*_{ex}$ as a function of temperature T for three values of applied electric field (F = 0 kV/cm, (solid lines) 40 kV/cm, (dashed lines) 80 kV/cm, (dotted lines)).

In order to have a global picture about the combined effect of the electric field and temperature on the exciton binding energy, we have shown, in Figure 5, the variation of the exciton binding energy in cylindrical QD as a function of applied electric field F and temperature T. From this figure, one can see clearly that the influence of the electric field on the binding energy is more obvious than the temperature. These results show that the binding energy depends strongly on the electric field as well as the temperature.

Figure 6 shows the variation of the stark shift as a function of electric field strength for two different dot height in a cylindrical $Ga_{(1-x)}Al_{(x)}As$ QD. We remark that the Stark shift decreases when the electric field strength increases and the stark effect becomes more important when increasing the dot height.

Figure 7 displays the variation of the electron–hole distance Z_{eh} as a function of the height H of the dot, with different electric field values (F = 0, 40 and 80 kV/cm) for $R = 1a^*_{ex}$ at zero and room temperature. It can be seen that long as the QD height augments, Z_{eh} increases and the influence of the electric field is more noticeable in those structures having larger sizes along the z-direction. On the other hand, the minima shown here can be explained with the fact that the wave functions penetrate deeper inside the barrier region, when the height of the QD becomes small enough. Moreover, the effect of temperature it also increase the distance electron-hole and this increase is more important for larger sizes of the cylinder height and for high electric field values. We can notice that for larger value of electric fields, the temperature effect becomes very low.

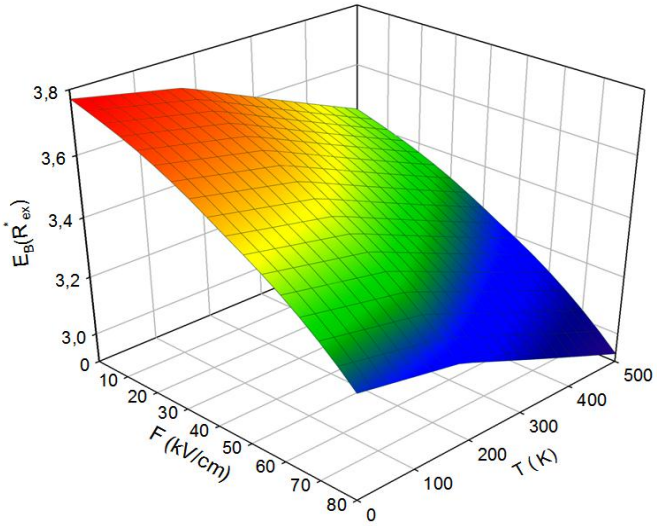

Figure 5: Variation of the exciton binding energy in a cylindrical $Ga_{(1-x)}Al_{(x)}As$ QD as a function of applied electric field F and temperature T for fixed radius $R = 1a^*_{ex}$ and height $H = 1a^*_{ex}$.

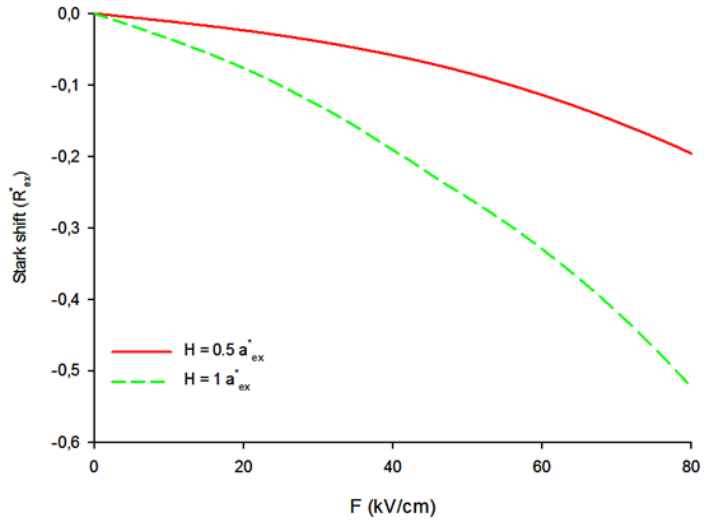

Figure 6: Variation of the stark shift as a function of electric field strength for two different dot height in a cylindrical $Ga_{(1-x)}Al_{(x)}As$ QD quantum dot at zero temperature.

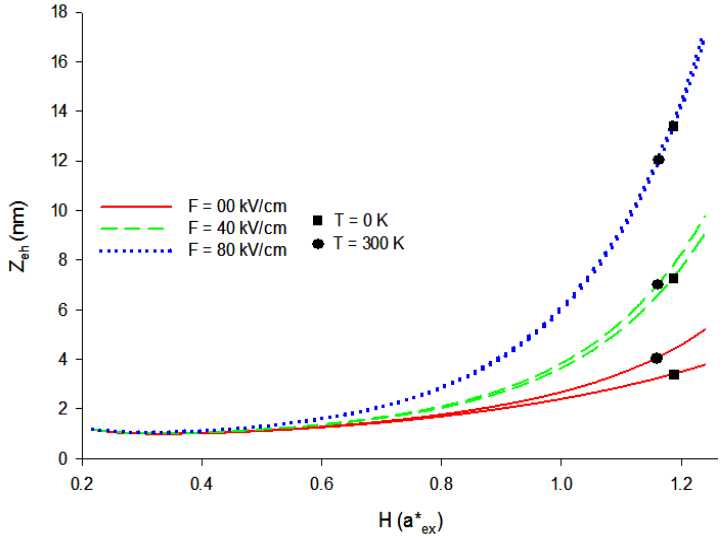

Figure 7: The electron–hole distance in a cylindrical $Ga_{(1-x)}Al_{(x)}As$ QD as a function of the QD height for fixed values of the radius $R = 1a^*_{ex}$,and three values of applied electric field (F = 0 kV/cm, (solid lines) 40 kV/cm, (dashed lines) 80 kV/cm, (dotted lines)) at zero and room temperature.

To make the above-mentioned results more clear, we have plotted the variation of the electron–hole distance versus the electric field and temperature for fixed radius $R = 1a_{ex}^{*}$ and height $H = 1a_{ex}^{*}$ in Figure8. In this figure, we remark that the electron–hole distance increases with increasing the applied electric field. Furthermore, regarding the effect of temperature, it is seen that the electron–hole distance increases linearly with increasing the temperature for each electric field value. The effect of temperature remains less important compared to the electric field effect. More especially, for large values of electric field (80 kV/cm) the temperature effect becomes negligible.

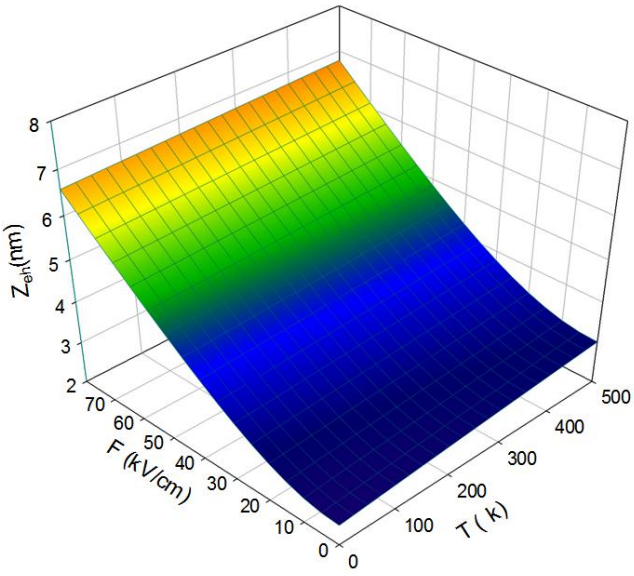

Figure 8: Variation of the electron–hole distance in a cylindrical $Ga_{(1-x)}Al_{(x)}As$ QD as a function of applied electric field F and temperature T for fixed radius $R = 1a_{ex}^{*}$ and height $H = 1a_{ex}^{*}$.

Figure 9 displays the variation of photoluminescence energy transition as a function of the dot height for different values of the electric field and temperature. The inset figure shows the interband emission energy as a function of applied electric field for the dot height $H = 1a_{ex}^{*}$ at zero and room temperature (T= 0 and 300 K). It is noted that the photoluminescence energy transition decreases monotonically as the dot height is increased. This is due to the confinement of electron–hole with respect to z axe when the dot height is increased. It is also shown that the photoluminescence energy transition decreases when increasing electric field and temperature, but the effect of temperature is less important than the effect of electric field. More especially, the effect of the electric field becomes more important at room temperature than at low temperature limit.

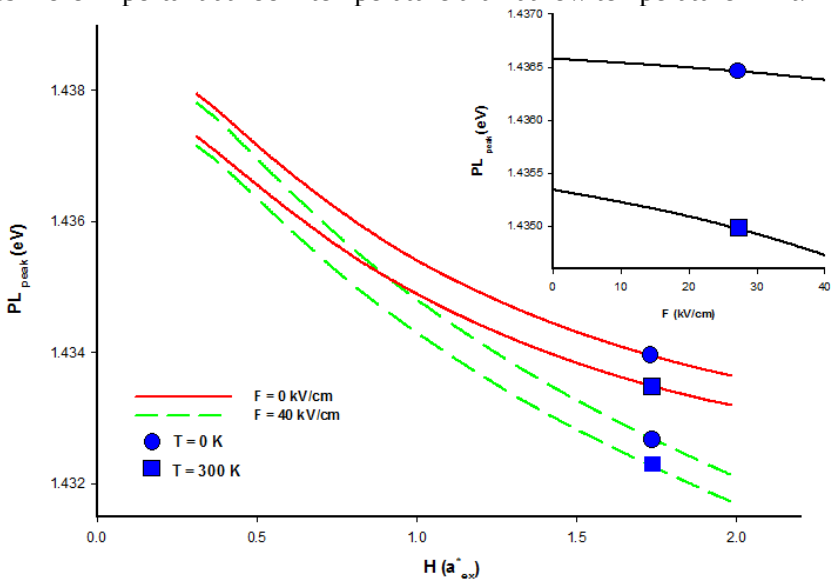

Figure 9: Variation of photoluminescence energy transition as a function of the dot height for different values of electric field and temperature. The inset figure shows the photoluminescence transition energy as a function of electric field for fixed $H = 1a_{ex}^{*}, R = 1a_{ex}^{*}$ at zero and room temperature.

Conclusions

In this work, we have studied the role of electric field and temperature on the binding energy corresponding to the ground state for an exciton in $GaAs/Ga_{(1-x)}Al_{(x)}As$ cylindrical QD following a variational procedure within the effective mass approximation. In general, augmenting the dimensions of the QD leads to a decrease in the exciton binding energy due to the reduction of carriers confinement. Our findings show that, after application of the electric field and temperature, the existence of an additional diminishing of the binding energy induced by the selective spatial separation of confined electrons and holes is appeared and the corresponding weakening of the Coulombic interaction. We have also calculated the electron–hole distance under the effect of applied electric field and temperature and we have remarked that, when the effect of electric field and temperature increase the distance electron-hole increases, but the effect of temperature remains less important compared to the electric field effect. Further, we have discussed the dependence of the exciton-related photoluminescence energy transition on QD size under the action of an applied electric field and temperature. The same decreasing behavior is observed for this physical parameter, and can be explained as well by the properties of the electron and hole confinement, via the corresponding modifications of the expected value of the distance between electron and hole, due to the changes in the dot's geometry and/or the applied electric field and temperature. These theoretical results show that in experimental studies of electronic, transport and optical properties of $Ga_{(1-x)}Al_{(x)}As$ nanostructures such as QDs, the effects of, applied electric field and temperature, on the exciton should be exploited. We hope that our work can stimulate forthcoming theoretical and experimental investigations in this attracting research area.

References

1. He, L. Xie,W., *Superlatt. Microstruct*. 47 (2010) 266.
2. Rezaei, G. Vaseghi, B. Ebrahimi, J., *Superlatt. Microstruct.* 49 (2011) 591.
3. Mughnetsyan, V. N. Barseghyan, M. G. Kirakosyan, A., *Superlatt. Microstruct*. 44 (2008) 86.
4. Tangarife, E. Duque, C. A., *Phys. Status Solidi B.* 247 (2010) 1778.
5. Fatemidokht, A. Askari, H. R., *Optics and Laser Technology*. 45 (2013) 684.
6. Saravanan, S. JohnPeter, A. Lee, C. W., *Physica E.* 67 (2015) 99.
7. Sangeetha, R. John Peter, A. Lee, C. W., *Superlatt. Microstruct.* 66 (2014) 54.
8. E. Aksahin, E. Ustoglu, V. Unal, Tomak., *Physica E.* 74 (2015) 258.
9. Shi, L. Yan, Z. W., *Superlatt. Microstruct.* 94 (2016) 204.
10. Khordad, R. Gharaati, A. Haghparast, M., *Curr. Appl. Phys*. 10 (2010) 199.
11. Harada, Y. Kasamatsu, N. Watanabe, D. Kita, T., *Phys. Rev. B.* 93 (2016) 115303.
12. Ozfidan, I. Korkusinski, M. Hawrylak, P., *Phys. Rev. B.* 91 (2015) 115314.
13. Kim, S. M. Yang, H. S., *Curr. Appl. Phys*. 11 (2011) 1249.
14. Kim, I. Kiba, T. Murayama, A. Song, J. D. Kyhm, K., *Curr. Appl. Phys.*15 (2015) 733.
15. Bautista, J. E. Q. Lyra, M. L. Lima, R.P.A., *Photonic. Nanostruct.* 11 (2013) 8.
16. Harris, L. Mawbray, L. D. Skolinick, M. S. Hopkinson, M. Hill, G., *Appl. Phys. Lett*. 73 (1998) 969.
17. Maimon, S. Finkman, E. Bahir, G. S. Schacham, S. E. Garsia, J. E. Petroff, P. M., *Appl. Phys. Lett.* 73 (1998) 2003.
18. Lundstrom, T. Schoenfeld, W. Lee, H. Petroff, P. M., *Science.* 286 (1999) 2312.
19. Bimberg, D. Grundmann, M. Ledenstov, N. N., *Quantum Dot Heterostructures, Wiley*, London, 1999.
20. Le Goff, S. Stébe´, B., *Phys. Rev. B.* 47 (1993) 1383.
21. Wang, G. Guo, K., *J. Phys. Condens. Matter*. 13 (2001) 8197.
22. Szafran, B. Chwiej, T. Peeters, F.M. Bednarek, S. Adamowski, J. Partoens, B., *Phys. Rev B.* 71 (2005) 205316.
23. Chwiej, T. Bednarek, S. Adamowski, J. Szafran, B. Peeters, F.M. *J. Lumin.* 112 (2005) 122.
24. Szafran, S. Peeters, F. M. Bednarek, S., *Phys. Rev. B* 75 (2007) 115303.
25. Barticevic, Z. Pacheco, M. Duque, C. A. Oliveira, L. E., *Eur. Phys. J. B* 56 (2007) 303.
26. Szafran, B Barczyk, E Peeters, F. M. Bednarek, S., *Phys. Rev. B.* 77 (2008) 115441.
27. Wang, D. Jin, G. Zhang, Y. Ma, Y., *J. Appl. Phys.* 105 (2009) 063716.
28. Erdogan, I. Akankan, O. Akbas, H ., *Superlatt. Microstruct*. 59 (2013) 13.
29. Yuan, J. H. Zhang, Y. Guo, X. Zhang, J. Mo, H., *Physica E.* 68 (2015) 232.

30. Li, X. J. Chang, K., *Appl. Phys. Lett.* 92 (2008) 251114.
31. Reimer, M. E. Korkusinski, M. Dalacu, D. Lefebvre, J. Lapointe, J. Poole, P. J. Aers, G. C. Mc Kinnon, W. R. Hawrylak, P. Williams, R. L., *Phys. Rev. B* 78 (2008) 195301.
32. Stokker-Cheregi, F. Vinattieri, A. Feltin, E. Simeonov, D. Levrat, J. Carlin, Butté, R. Grandjean, N. Gurioli, M., *Appl. Phys Lett.* 93 (2008) 152105.
33. Wang, D. Jin, G. J. Zhang, Y. Ma, Y. Q., *J. Appl. Phys.*105 (2009) 063716.
34. Luo, J. W. Li, S. S. Xia, J. B. Wang, L. W., *Phys. Rev. B.* 71 (2005) 245315.
35. El Moussaouy, A. Bria, D. Nougaoui, A., *Physica B.* 370 (2005) 178.
36. El Moussaouy, A. Ouchani, N. El Hassouani, Y. Benami, A., *Surface Science.* 624 (2014) 95.
37. El Moussaouy, A. Ouchani, N *Physica B.* 436 (2014) 26.
38. El Moussaouy, A. Ouchani, N. El Hassouani, Y. Abouelaoualim, D., *Superlatt. Microstruct.* 73 (2014) 22.
39. Rezaei, G. Vaseghi, B. Ebrahimi, J., *Superlatt. Microstruct.* 49 (2011) 591.
40. Mendoza, C. I. Vazquez, G. J. del Castillo-Mussot, M. Spector, H., *Phys. Rev. B* 71 (2005) 075330.
41. Vartanian, A. L. Vardanyan, A. Kazaryan, M., *Physica E.* 40 (2008) 1513.
42. He, L. Xie, W., *Superlatt. Microstruct.* 47 (2010) 266.
43. Dane, C. Akbas, H. Minez, S. Guleroglu, A., *Physica E.* 42 (2010) 1901.
44. Barseghyan, M. G., *Physica E.* 69 (2015) 219.
45. Niculescu, E. C. Cristea, M. Spandonide, A., Superlatt. Microstruct. 63 (2013) 1.
46. Xia, C. Zeng, Z. Liu, Z. S. Wei, S.Y., *Physica B.* 405 (2010) 2706.
47. Duque, C. M. Barseghyan, M. G. Duque, C.A., *Physica B Condensed Matter*. 404 (2009) 5177.
48. Sali, A. Satori, H., *Superlatt.Microstruct*. 69 (2014) 38.
49. Leon, H. Marin, J. L. Riera, R., *Physica E.* 27 (2005) 385.
50. Mora-Ramos, M. E. Duque, C. A., *Physica B.* 407 (2012) 2351.
51. Xie, W., *Physica B.* 407 (2012) 1134.
52. Man, M. T. Lee, H. S., *Current Appl. Phys.* 14 (2014) S107.
53. Duque, C. M. Mora-Ramos, M. E. Duque, C. A., *Physica B.* 407 (2012) 4773.
54. Oyoko, H. O. Duque, C. A. Porras-Montenegro, N., J. *Appl. Phys.* 90 (2001) 819.
55. Kasapoglu, E. *Phys. Lett. A.* 373 (2008) 140.

(2017) ; http://www.jmaterenvironsci.com/